First Year Activity Report

Giovanni Scala

Dottorato di Ricerca in Fisica, XXXIII ciclo

Dipartimento Interateneo di Fisica "M. Merilin"

Research activity

My first year in the research field has focused in the Classical and Quantum Optics. I have started from the optical coherence theory and the plenoptic imaging studying the properties of fluctuating electromagnetic fields, paying attention mainly to the optical region of the electromagnetic spectrum. It seems hardly necessary to stress that every electromagnetic field found in nature has some fluctuations associated with it. Even though these fluctuations are usually much too rapid to be observed directly, one can deduce their existence from suitable experiments that provide information about correlations between the fluctuations at two or more space-time points. The simplest manifestations of correlations in optical fields are the well known interference effects that arise when two light beams that originate from the same source are superposed. With the availability of modern light detectors and electronic circuitry of very short resolving time, other types of correlations in optical fields began to be studied in more recent times. These investigations led to a systematic classification of optical correlation phenomena and the complete statistical description of optical fields. The area of optics concerned with such questions is what we call optical coherence theory. The "second-order theory" provides the introduction of a precise measure of correlations between the fluctuating field variables at two space-time points and the formulation of dynamical laws which the correlation functions obey in the free space.

Correlation Plenoptic Imaging

My main contribution regards the Correlation Plenoptic Imaging (CPI), a novel imaging technique, that exploits classical and quantum correlations between intensity fluctuations in two light beams to perform the typical tasks of plenoptic imaging, namely refocusing out-of-focus parts of the scene, extending the depth

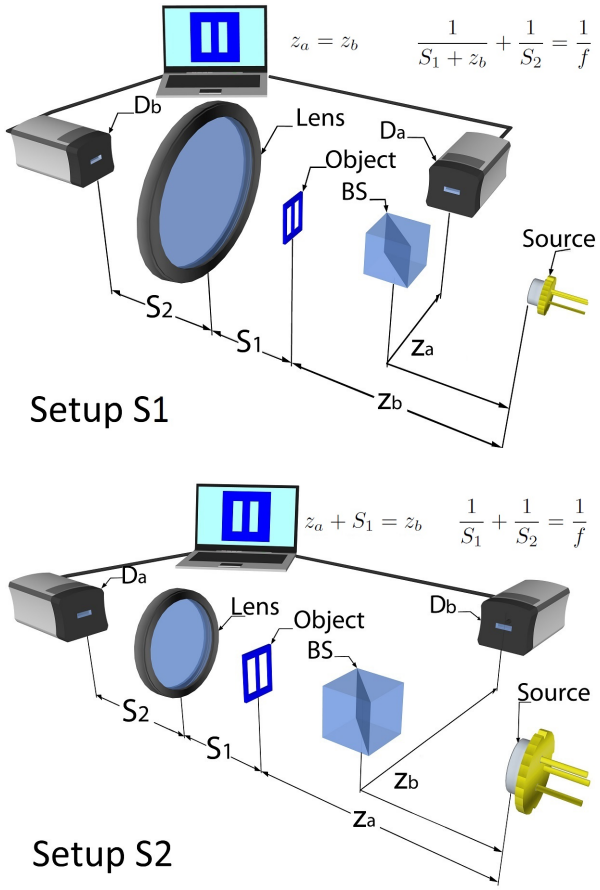

Figure 1: Schematic representation of two setups that enable to perform plenoptic imaging by measuring correlations of intensity fluctuations $\Delta i(\boldsymbol{\rho}_a)\Delta i(\boldsymbol{\rho}_b)$ between points on two spatially resolving detectors D_a and D_b.

of field, performing 3D reconstructions. In this framework, I have characterized the noise properties, in particular the signal-to-noise ratio, of two setups aimed at performing plenoptic imaging with intensity correlations measurements. Both setups are illuminated by chaotic light, split in two paths by a beam splitter, and feature a transmissive object and a lens of focal length f. In setup S1 (upper panel), the chaotic source is focused by the lens on the detector D_b, while the "ghost" image of the object emerges in correspondence of D_a from the average $\Gamma(\boldsymbol{\rho}_a, \boldsymbol{\rho}_b) = \langle \Delta i(\boldsymbol{\rho}_a)\Delta i(\boldsymbol{\rho}_b)\rangle$. Setup S2 (lower panel) is based on a different working principle: the image of the object is formed by the lens on D_a, while the image of the lens is retrieved in correspondence of D_b by averaging correlations. In both cases, correlated detection of the two images contains information on the direction of light in the setup, which provides the possibility

to recover the image of the object even the focusing conditions (namely, $z_b = z_a$ for S1, and $1/S_1 + 1/S_2 = 1/f$ for S2) are not matched. The common feature of the two setups, represented in Fig. 1, is the fact that light emitted by a chaotic source is split in two paths a and b by a beam splitter (BS), with an object placed in one of the paths, and is recorded at the end of each path by the high-resolution detectors D_a and D_b. More specifically, intensity patterns $i_A(\boldsymbol{\rho}_a)$ and $i_B(\boldsymbol{\rho}_b)$, with $\boldsymbol{\rho}_{a,b}$ the coordinate on each detector plane, are recorded in time to reconstruct the correlation function

$$\Gamma_{AB}(\boldsymbol{\rho}_a, \boldsymbol{\rho}_b) = \langle \Delta i_A(\boldsymbol{\rho}_a) \Delta i_B(\boldsymbol{\rho}_b) \rangle \,, \tag{1}$$

with $\Delta i_{A,B}(\boldsymbol{\rho}_{a,b}) = i_{A,B}(\boldsymbol{\rho}_{a,b}) - \langle i_{A,B}(\boldsymbol{\rho}_{a,b}) \rangle$. The expectation value in (1) must be evaluated on the source statistics, but it can be approximated by the time average of the product of intensity fluctuation, provided the source is stationary and ergodic [15]. The lens in S1 focuses the source on the detector D_b, while the lens appearing in S2 focuses the object on D_a. The role of the source is less intuitive: actually, when measuring second-order correlations, a chaotic source acts as a *focusing element* [12]. In our cases, as will be explained in more detail in the following, the source focuses the object on D_a in S1, and the lens on D_b in S2.

In both setups, the correlation function (1) at fixed $\boldsymbol{\rho}_b$ encodes multiple coherent images of the object. Each point $\boldsymbol{\rho}_b$ on the plane of detector D_b corresponds to a different point of view on the scene, and the images corresponding to different $\boldsymbol{\rho}_b$'s are generally shifted one with respect to the other. If the position of the object in each setup satisfies a specific focusing condition, the relative shift of such images vanishes, and one can integrate over the detector D_b to obtain a total incoherent image, with improved SNR. In all other cases, the images must be realigned before being piled up by integrating over D_b, following

$$\Sigma_{\mathrm{ref}}(\boldsymbol{\rho}_a) = \left\langle \sigma_{(\alpha,\beta)}(\boldsymbol{\rho}_a) \right\rangle , \tag{2}$$

with

$$\sigma_{(\alpha,\beta)}(\boldsymbol{\rho}_a) = \int \mathrm{d}^2 \boldsymbol{\rho}_b \Delta i_A(\alpha \boldsymbol{\rho}_a + \beta \boldsymbol{\rho}_b) \Delta i_B(\boldsymbol{\rho}_b). \tag{3}$$

The parameters (α, β), that are necessary to realign the coherent images, depend on the setup. he fluctuations of the observable (3) around their average $\Sigma_{\mathrm{ref}}(\boldsymbol{\rho}_a)$, namely

$$\begin{aligned} \mathcal{F}(\boldsymbol{\rho}_a) &= \left\langle \sigma_{(\alpha,\beta)}(\boldsymbol{\rho}_a)^2 \right\rangle - \left\langle \sigma_{(\alpha,\beta)}(\boldsymbol{\rho}_a) \right\rangle^2 \\ &= \int \mathrm{d}^2 \boldsymbol{\rho}_{b1} \mathrm{d}^2 \boldsymbol{\rho}_{b2} \Phi(\boldsymbol{\rho}_a, \boldsymbol{\rho}_{b1}, \boldsymbol{\rho}_{b2}), \end{aligned} \tag{4}$$

with Φ a positive function related to the local fluctuations of intensity correlations [compare with the definition of (3), to obtain an estimate of the signal-to-noise ratio related to the refocused images retrieved in S1 and S2. We have achieved interesting properties of the signal-to-noise ratio for the setups S1

and S2, finding that the results obtained for the latter are generally more advantageous than the former. In the focused case, S2 is characterized by the suppression of background noise, that, on the other hand, is a typical feature affecting the ghost image obtained in S1. Moreover, noise in S1 increases with improving resolution on the object entailing a trade-off between resolution and SNR trade-off. In the out-of-focus case, background noise is present in both configurations. However, in S1 it depends on small quantities, namely the ratios between the area of an effective resolution cell and the total area of the object. In S2, instead, we find that the SNR depends also on the ratio between the effective lens area and the one of the object, a quantity that is not necessarily small. Therefore, we expect that a smaller number of frames is needed to achieve the same resolution in S2 compared to S1. The outcomes provide the experimenter with rules to determine the scaling of the SNR with the number of frames, and consequently to fix the number of frames needed for a fast and accurate imaging of the scene. The problem of optimizing the acquisition time is particularly relevant if unconventional sources like X rays [13, 14], characterized by additional difficulties in retrieving intensity correlations, will be employed to perform CPI.

Turbulence free Model

The study in the previous section apply the ghost imaging effect, which is a key concept even for the turbulence-free imaging. According to the same framework of equation I have studied some mathematical model in order to characterize the turbulence in the optical systems[8]. Roughly speaking these configurations are not sensible to the refraction index fluctuations which usually introduce such noise in the images. Nonetheless, just specific setups satisfied these properties as it is summarized in the Fig.2. The transmission turbulence function introduce a phase variation due to the Reyleigh scatter of the light with the atmosphere

$$T(\boldsymbol{\rho}) = e^{i\phi(\boldsymbol{\rho})} = 1 + i\phi(\boldsymbol{\rho}) - \frac{1}{2}\phi^2(\boldsymbol{\rho}) + o\left(\phi^2\right),$$

it is modelized upon a plan with coordinate $\boldsymbol{\rho} = (x, y)$ ruled by the following correlation phase function in two points of the tubulence plan

$$\langle \phi(\boldsymbol{\rho}_1)\,\phi(\boldsymbol{\rho}_2)\rangle_T = \sigma_\phi^2 e^{-\frac{(\boldsymbol{\rho}_1-\boldsymbol{\rho}_2)^2}{2\sigma_T^2}},$$

with $\sigma_\phi$represents the intensity of the correlation and σ_T the correlation length of the two considered points. Since the scattering is isotropic, the mean value of difference processes at any point $\boldsymbol{\rho}$ is $\langle \phi(\boldsymbol{\rho})\rangle_T = 0$. Therefore up to the second order we have $T(\boldsymbol{\rho}) = 1 + i\langle\phi(\boldsymbol{\rho})\rangle_T - \frac{1}{2}\langle\phi^2(\boldsymbol{\rho})\rangle_T = 1 - \frac{\sigma_\phi^2}{2}$ and the correlation of two point in the transmission function, which is the crucial term in the second

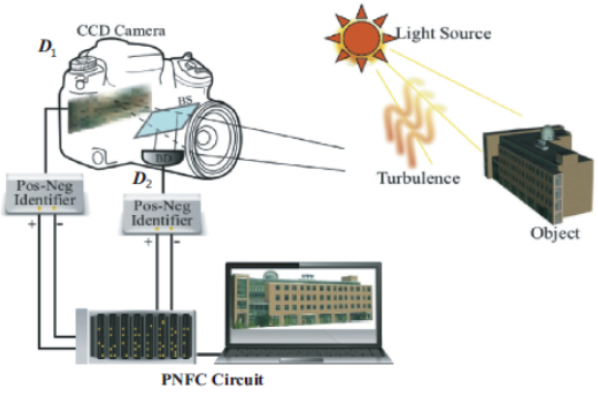

Figure 2: Schematization of a turbulence-free camera. The light from the building across the turbulence which perturbs the phase of the wavefield, but at the second order it goes away.[8]

order imaging reads

$$\begin{aligned}\langle T^*(\boldsymbol{\rho}_1)\,T(\boldsymbol{\rho}_2)\rangle_T =& \langle e^{i(\phi(\boldsymbol{\rho}_1)-\phi(\boldsymbol{\rho}_2))}\rangle_T \\ =& 1-\sigma_\phi^2+\langle\phi(\boldsymbol{\rho}_2)\,\phi(\boldsymbol{\rho}_1)\rangle_T \\ =& 1-\sigma_\phi^2+\sigma_\phi^2 e^{-\frac{(\boldsymbol{\rho}_1-\boldsymbol{\rho}_2)^2}{2\sigma_T^2}}.\end{aligned}$$

My efforts consists to generalize the PCI protocol in the turbulence-free regime.

Two-level systems with broken inversion symmetry

Besides the topics outlined in the preceding part of this report, I am recently studying the Jaynes-Cummings model (JC). It is a theoretical model in quantum optics for a system of a two-level atom interacting with a quantized mode of an optical cavity. In particular, I am studying the presence of a non trivial emission at the Rabi frequency with broken symmetry in the diagonal terms of dipole moment. Analytical results for the time-averaged radiation intensity in relevant physical situations are obtained at the first perturbative order in the symmetry violation parameter. Since the Rabi frequency is proportional to the strength of the coupling with the electromagnetic field, the effect can be used for frequency-tuned parametric amplification and generation of electromagnetic waves. Beyond JC, I am also working on the spontaneous emission as a coupling with the electromagnetic field of the vacuum during my summer period in Poland attending to TAPS program (The Toruń Astrophysics and Physics Summer Project), focusing on the differences in the spontaneous emission for a two-level quantum system when are present the diagonal terms of the dipole matrix attempting different approaches, as well as, the Heisenberg picture, the resolvent

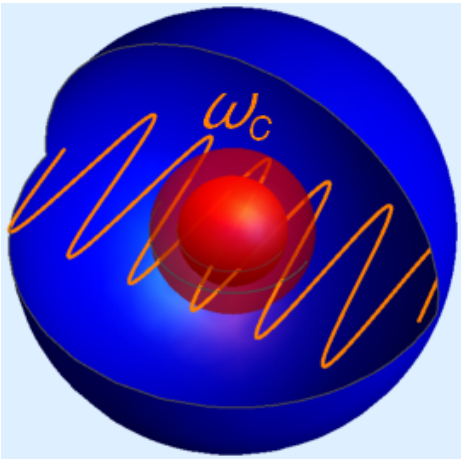

Figure 3: Schematic representation of Rydberg atom in the cavity coupled with an external electromagnetic field. *(this image is realized with WolframMathematica)*

method and the master equation consider the external electromagnetic field as a reservoir. Basically the model is the following

$$H^{od} = H_a + H_f + H_I^{od}$$

where for $t = 0$ we have

$$H_a = \hbar\omega_A \sigma^\dagger \sigma$$

$$H_f = \hbar \int d^3r \int d\omega\omega \boldsymbol{f}^\dagger(r,\omega)\boldsymbol{f}(r,\omega)$$

$$H_I^{od} = -\boldsymbol{d}\cdot\boldsymbol{E}\left(r_A\right)\Big|_{d_e=d_g=0} = -\boldsymbol{d}\left(\sigma+\sigma^\dagger\right)\cdot\boldsymbol{E}\left(\boldsymbol{r}_A\right)$$

$$H_I^{d} = -\boldsymbol{d}\cdot\boldsymbol{E}\left(r_A\right)\Big|_{d_e\neq d_g} = -\left(\frac{\boldsymbol{d}_e+\boldsymbol{d}_g}{2}\boldsymbol{I}+\frac{\boldsymbol{d}_e-\boldsymbol{d}_g}{2}\sigma_z\right)\cdot\boldsymbol{E}\left(\boldsymbol{r}_A\right)$$

with

$$E_k\left(\boldsymbol{r}_A,t\right) = \int_{-\infty}^{\infty} d\omega i\sqrt{\frac{\hbar}{\pi\epsilon_0}}\frac{\omega^2}{c^2}\int d^3\boldsymbol{r}'\sqrt{\Im\epsilon\left(\boldsymbol{r}',\omega\right)}G_{kj}\left(\boldsymbol{r}_A,\boldsymbol{r}',\omega\right)f_j\left(\boldsymbol{r}',\omega,t\right),$$

where $f(\boldsymbol{r},\omega,t)$ satisfied the bosonic operator commutation relation

$$\left[f_{\boldsymbol{k}}\left(\boldsymbol{r},\omega\right), f_{\boldsymbol{k}'}\left(\boldsymbol{r}',\omega'\right)\right] = \delta_{\boldsymbol{k}\boldsymbol{k}'}\delta\left(\boldsymbol{r}-\boldsymbol{r}'\right)\delta\left(\omega-\omega'\right) \tag{5}$$

. One of the most important outcome is obtained thank to the resolvent method.

The dressed excited state reads

$$R_e(z) = \sum_{|s,i\rangle} \frac{\langle e;0|H_{int}|s,i\rangle\langle s,i|H_{int}|e;0\rangle}{z - E_i} \tag{6}$$

After a straightforward calculation the final result is

$$R_e(E) = \hbar\Delta_e^{(d)}(E) - i\hbar\frac{\Gamma_e^{(d)}(E)}{2} + \hbar\Delta_e^{(od)}(E) - i\hbar\frac{\Gamma_e^{(od)}(E)}{2}. \tag{7}$$

The damping term is particular interesting because depends on the diagonal terms of the dipole matrix, that we have introduce in the our model beyond the JC model. As final outcome I have achieved the following expression

$$\Gamma_e^{(d)}(E) = d_{e_m} d_{e_k} \frac{1}{2\epsilon_0\hbar c^2} \frac{(E_e - E)^2}{\hbar^2} \Im G_{mk}\left(\boldsymbol{r}_A, \boldsymbol{r}_A, \frac{(E - E_e)}{\hbar}\right)\theta(E - E_e). \tag{8}$$

The quantity G is the *Green tensor propagator* which describes the propagation of the external electromagnetic field in a no homogeneous and isotropic medium, defined by the following differential equation

$$\left[\partial_i\partial_m - \delta_{im}\left(\partial^2 + q^2(\omega)\right)\right] G_{ij}(\boldsymbol{r}, \boldsymbol{r}', \omega) = \delta_{mj}\delta(\boldsymbol{r} - \boldsymbol{r}') \tag{9}$$

The most general solution is

$$\begin{aligned}\mathbf{G}(\boldsymbol{\rho}, \omega) =& \frac{1}{(2\pi)^3 q^2(\omega)} \int_0^\infty dk \int_0^\pi d\theta \frac{-e^{ik\rho\cos\theta} k^4}{k^2 - q^2(\omega)} \sin\theta \\ &\times \int_0^{2\pi} \begin{pmatrix} \sin^2\theta\cos^2\phi - q^2/k^2 & \sin^2\theta\sin\phi\cos\phi & \sin\theta\cos\theta\cos\phi \\ \sin^2\theta\sin\phi\cos\phi & \sin^2\theta\sin^2\phi - q^2/k^2 & \sin\theta\cos\theta\sin\phi \\ \sin\theta\cos\theta\cos\phi & \sin\theta\cos\theta\sin\phi & \cos^2\theta - q^2/k^2 \end{pmatrix} d\phi.\end{aligned} \tag{10}$$

Training activities

During the first year of my PhD I attended the following courses:

- Management and knowledge of European research model and promotion of research results by dr. D'Orazio (completed);
- How to prepare a technical speech in English by prof. White (completed);
- Programing with Python for Data Science by dr. Diacono (completed);
- Introduction to C++ programming by dr. Cafagna (final exam to be taken);
- Linear Stability analysis by prof. Gonnella (course still in progress to date);

- Differential equations and physical phenomena by prof. Pascazio (completed);
- States, observables and Evolution by prof. Facchi (completed);
- Atom-photon interactions by dr. Pepe (completed).

I also attended the following schools and conferences:

- *Statistical Mechanics & Field Theory*, Bari, 13–15 December 2017;
- *Current Problems in Theoretical Physics*, Vietri sul Mare (SA), 24–25 March 2018;
- *Information Geometry, Quantum Mechanics and Applications*, San Rufo (SA), 25–30 June 2018, with presentation of the talk "Two-Level Quantum Systems with Broken Inversion Symmetry";
- *XXX National Seminar of Nuclear and Subnuclear Physics "Francesco Romano"*, Otranto (LE), 5–12 June 2018
- TAPS (The Toruń Astrophysics / Physics Summer Program), Toruń (Poland), August 2018, with the project "Light interactions to asymmetric quantum systems"
- Italian Quantum Information Science conference, Catania, 17–20 September 2018, with presentation of the poster "Two-Level Quantum Systems with Broken Inversion Symmetry".

References

[1] C. Cohen-Tannoudji, J. Dupont-Roc, and G. Grynberg, *Atom-Photon Interactions: Basic Processes and Applications* (Wiley, Chichester, 1998)

[2] R. Ng, M. Levoy, M. Brédif, G. Duval, M. Horowitz, and P. Hanrahan, "Light field photography with a hand-held plenoptic camera," Stanford University Computer Science Tech Report CSTR 2005-02, 2005.

[3] C. Wu, J. Ko, and C. C. Davis, "Imaging through strong turbulence with a light field approach," Opt. Express **24**, 11975 (2016).

[4] M. D'Angelo, F. V. Pepe, A. Garuccio, and G. Scarcelli, "Correlation Plenoptic Imaging," Phys. Rev. Lett. **116**, 223602 (2016).

[5] F. V. Pepe, G. Scarcelli, A. Garuccio, and M. D'Angelo, "Plenoptic imaging with second-order correlations of light," Quantum Meas. Quantum Metrol. **3**, 20 (2016).

[6] F. V. Pepe, F. Di Lena, A. Garuccio, G. Scarcelli, and M. D'Angelo, "Correlation plenoptic imaging with entangled photons," Technologies–Open Access Multidisciplinary Engineering Journal **4**, 17 (2016).

[7] F. V. Pepe, F. Di Lena, A. Mazzilli, E. Edrei, A. Garuccio, G. Scarcelli, and M. D'Angelo, "Diffraction-Limited Plenoptic Imaging with Correlated Light," Phys. Rev. Lett. **119**, 243602 (2017).

[8] Y. Shih,The Physics of Turbulence-Free Ghost Imaging, Technologies2016, 4, 39

[9] T. B. Pittman, Y. H. Shih, D. V. Strekalov, and A. V. Sergienko, "Optical imaging by means of two-photon quantum entanglement," Phys. Rev. A **52**, R3429 (1995).

[10] A. Gatti, E. Brambilla, M. Bache, and L. A. Lugiato, "Ghost imaging with thermal light: comparing entanglement and classical correlation," Phys. Rev. Lett. **93**, 093602 (2004).

[11] R. S. Bennink, S. J. Bentley, R. W. Boyd, and J. C. Howell, "Quantum and Classical Coincidence Imaging", Phys. Rev. Lett. **92**, 033601 (2004).

[12] G. Scarcelli, V. Berardi, and Y. Shih, "Can two-photon correlation of chaotic light be considered as correlation of intensity fluctuations?," Phys. Rev. Lett. **96**, 063602 (2006).

[13] D. Pelliccia, A. Rack, M. Scheel, V. Cantelli, and D. M. Paganin, "Experimental X-Ray Ghost Imaging," Phys. Rev. Lett. **117**, 113902 (2016).

[14] R. Schneider *et al.*, "Quantum imaging with incoherently scattered light from a free-electron laser," Nat. Phys. **14**, 126 (2018).

[15] L. Mandel, E. Wolf, *Optical Coherence and Quantum Optics* (Cambridge University Press, Cambridge, 1995).

[16] M. O. Scully and M. S. Zubairy, *Quantum Optics* (Cambridge University Press, Cambridge, 1997).

[17] M. N. O'Sullivan, K. W. C. Chan, and R. W. Boyd, "Comparison of the signal-to-noise characteristics of quantum versus thermal ghost imaging," Phys. Rev. A **82**, 053803 (2010).

[18] Bruce W. Shore & Peter L. Knight (1993): The Jaynes-Cummings Model, Journal of Modern Optics, 40:7, 1195-1238

[19] R. R. Puri and G. S. Agarwal, Phys. Rev. A **33**, 3610 (1986).

[20] G. Rempe, H. Walther, and N. Klein, Phys. Rev. Lett. **58**, (1987).

[21] O.V. Kibis et al., Tech. Phys. Lett. **31**,671 (2005)

[22] O.V. Kibis et al., Phys. Rev. Lett. **102**, 023601 (2009)